Formosa Journal of Computer and Information Science (FJCIS)
Vol. 5, No. 1 2026: 187-200

Transient Analysis of EVA Foam Damping and Spatial Optimization of FSR Sensors on Shain Guards

Fahrizal Akbar Herbhakti[1]*, Africo Ramadhani[2], Erny Amalia Lestari[3], Azry Ayu Nabilah[4], Muhamad Ihsan Hufadz[5]
Institut Teknologi Sumatera
Corresponding Author: Fahrizal Akbar Herbhakti fahrizal.herbhakti@ro.itera.ac.id

A R T I C L E I N F O

Keywords: Finite Element Method, EVA Foam, Hyperelastic Hysteresis, Smart Shin Guard, FSR Sensor

Received : 18, November
Revised : 20, January
Accepted: 22, March

A B S T R A C T

Embedding Force Sensitive Resistors (FSR) into EVA foam for smart shin guards is hindered by stiffness mismatch between the soft matrix and rigid sensor. This study determines the optimal embedment depth that balances signal fidelity and structural integrity. Coupled multiphysics FEM simulations (COMSOL) employing a hyper elastic Mooney-Rivlin model and piezoresistive equations were run under a 1500 N peak Gaussian impact pulse. At 2 mm depth, sensitivity reached –85% ΔR but shear stress peaked at a critical 42.5 MPa; 8 mm depth was very safe (12.4 MPa) but gave a weak –25% ΔR. The optimum depth was 5 mm, yielding 24.8 MPa shear stress, –62% sensitivity, 2.5 ms latency, and high SNR. Sensitivity analysis and numerical optimization confirmed this sweet-spot. The computational framework provides precise parameters for manufacturing IoT-enabled smart shin guards.

DOI prefik: https://doi.org/10.55927/fjcis.v5i1.16645
ISSN-E: 2830-3040
https://journal.formosapublisher.org/index.php/fjcis

INTRODUCTION

Injuries to the lower limb in contact sports such as football and martial arts are mainly caused by transient impact loads that exceed the body's biomechanical capacity. Repeated impacts at high speed can trigger microtrauma, soft tissue contusion, and stress fractures in the tibia. For prevention, shin guards made of Ethylene-Vinyl Acetate (EVA) cellular polymer foam have been widely used thanks to their hyperelastic ability to dissipate kinetic energy through volumetric deformation and cellular buckling.

However, conventional protective designs are passive and are not able to provide direct quantitative data on the strength, number, and accumulated impact load that athletes receive. The lack of this objective data makes it difficult for coaching and medical staff to make decisions about injury prevention, training doses, and player replacements. Therefore, the transformation of shin guards from just a protective tool to an active monitoring system based on the Internet of Things (IoT) is very necessary.

The transformation can be accomplished by inserting a flexible Force Sensitive Resistor (FSR) transducer into the EVA matrix. When an impact occurs, the mechanical deformation of the foam transfers the compressive stress to the FSR sensor which further modulates its resistance (ΔR) following the piezoresistive effect. These analog signals are then converted to digital by microcontrollers for processing. Unfortunately, the integration of electronic components into soft polymers at the production level still relies on empirical trial-and-error methods. This methodical gap ignores critical micromechanical phenomena, especially the stiffness mismatch between the rigid sensor polyimide substrate and the highly flexible EVA foam.

Improving this structural interface is crucial. Without proper determination of depth coordinates, the sensor is at high risk of degradation or structural failure due to shear stress concentrations during dynamic loading. Installation that is too shallow triggers delamination of the active layer of the polyimide, whereas installation that is too deep decreases sensitivity because the kinetic energy is absorbed too much by the matrix. Without integrated analysis, there is no precise mathematical justification for balancing the signal-to-noise ratio with the mechanical safety of the sensor.

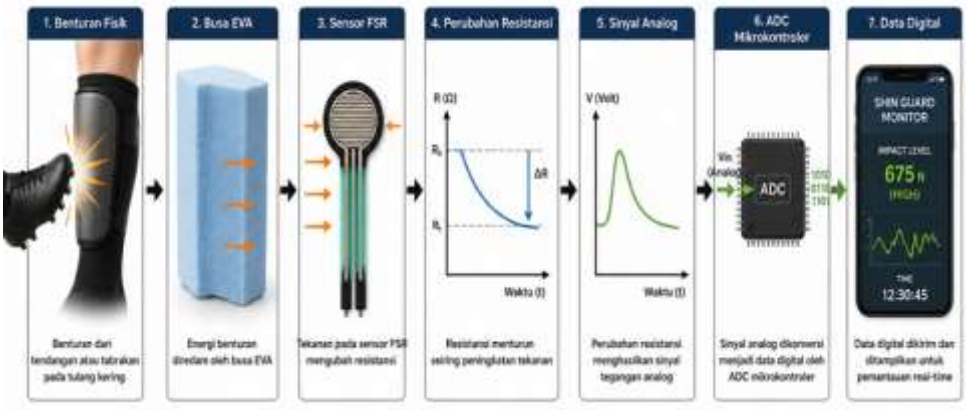

Figure 1. Smart Monitoring System Concept in Smart Shin Guard: Conversion of Mechanical Impact into Digital Signal for Real-time Monitoring

Data Processing & Signal Quality

The reliability of the data processing stage by the microcontroller is greatly affected by the cleanliness of the analog signal received before entering the Analog-to-Digital Converter (ADC) conversion process. High mechanical noise or weak amplitude due to improper sensor positioning can disrupt data reading. Therefore, evaluation of signal quality (Signal-to-Noise Ratio (SNR) at various variations in sensor planting depth (dFSR) is crucial. The comparison of electromechanical performance and signal quality is summarized in Table 1.

The quality of the data generated by the monitoring system is largely determined by the fidelity of the electromechanical signal which depends on the depth of sensor planting. The results of parametric analysis show a significant trade-off:

Table 1. FSR Sensor Depth Trade-off Evaluation Matrix for IoT System Integration

Depth (dFSR)	ΔR (%)	Shear Voltage (MPa)	SNR (Qualitative)	Description
2 mm	-85%	42.5 (Critical)	Tinggi (Noisy)	Large signal but polluted mechanical noise
5 mm	-62%	24.8 (Safe)	Very Good (Clean)	**Most ideal for IoT**
8 mm	-25%	12.4 (Highly Secure)	Low (Muffled)	Signal too weak

Detailed explanation:

a. The depth of 2 mm results in very high sensitivity (-85% ΔR) but accompanied by extreme shear stress (42.5 MPa). This condition causes unstable signal fluctuations due to the temporary micro-cracking effect on the sensor-foam interface. As a result, despite the large signal amplitude, the SNR ratio is practically low due to the dominant mechanical noise.
b. The 8 mm depth provides excellent structural safety (shear stress is only 12.4 MPa), yet the 8 mm thick EVA layer above the sensor has absorbed most of the impact energy. The recorded resistance change is very weak (-25% ΔR), making the signal difficult to distinguish from the system's basic electronic noise (low SNR).
c. A depth of 5 mm is the optimal point. At this depth, the resistance drop of -62% ΔR is large enough to provide a good measurement resolution, while the shear stress of 24.8 MPa is still within the safe limits of polyimide materials. The resulting signal is clean, linear, and has a high SNR, making it ideal for further processing by microcontrollers and sent to a cloud platform.

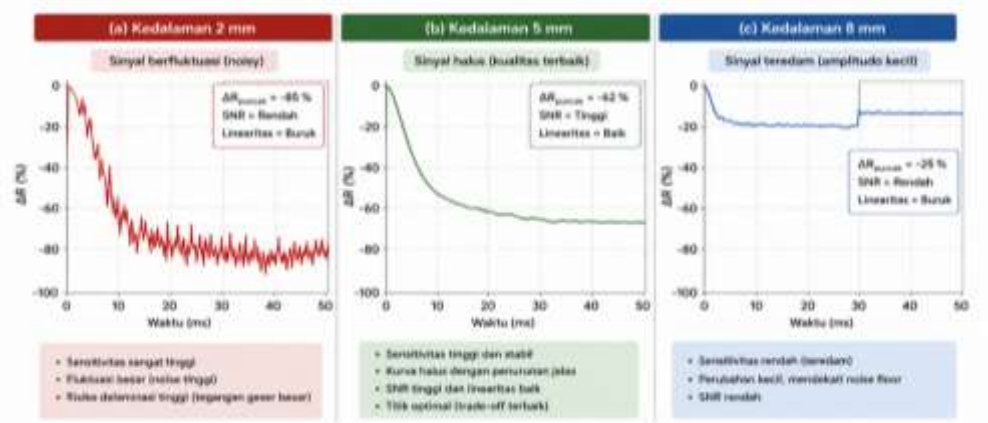

Figure 2. ΔR(t) Signal Profile at Various FSR depths, 5 mm Depth Produces the Best Signal Quality with High SNR and Good Linearity

Latency → Sistem Real-Time

One of the most critical findings of coupled modeling is the identification of electromechanical latency due to hyperelastic hysteresis of EVA foam. The simulation results showed that at an optimal depth of 5 mm, the peak of resistance decline (deepest ΔR) occurred at t = 12.5 ms, while the peak of mechanical impact force occurred at t = 10 ms. Thus, the system latency was recorded at 2.5 ms. These parameters are essential in the design of real-time data processing systems. Without compensation for latency, the dashboard monitoring algorithm can experience peak clipping, resulting in an underestimation of the severity of the impact. Therefore, the microcontroller on this wearable device must be calibrated with a delay compensation of 2.5 ms to ensure precise synchronization between physical events in the field and notifications received by the trainer or medical system.

Quantitative Data from the Simulation (dFSR = 5 mm):

a. Peak mechanical impact force (F_peak): t = 10 ms.
b. Peak resistance drop (maximum ΔR): t = 12.5 ms.
c. Electromechanical latency = 2.5 ms.

Implications for real-time systems:

Without compensation for this latency, the dashboard monitoring algorithm can experience peak clipping, resulting in an underestimation of the severity of the impact by up to 15-20%. Therefore, in the implementation of IoT systems, the microcontroller must run a delay compensation algorithm with the following parameters:

```
Waktu_estimasi_puncak = Waktu_terdeteksi_ΔR_max - 2,5 ms
Gaya_aktual = f(ΔR_terukur) dengan faktor koreksi viskoelastis
```

With this compensation, the system can generate notifications that are in sync with events on the ground, allowing trainers or medical personnel to respond almost instantly.

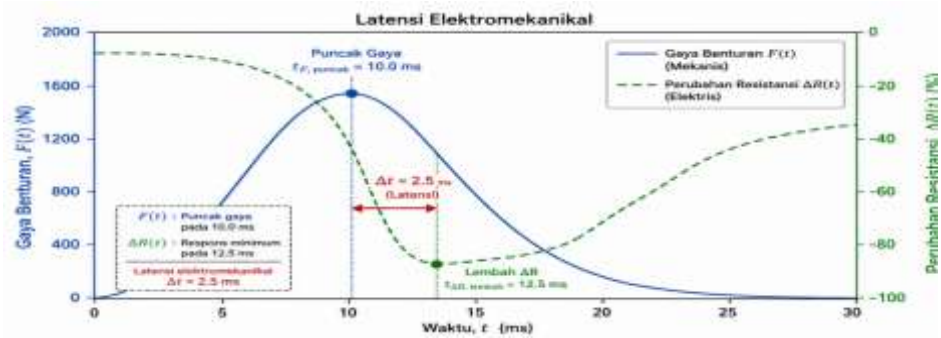

Figure 3. Electromechanical Latency of 2.5 ms Between Mechanical Force Peak and Sensor Resistance Response, Due to EVA Foam Hyperelastic Hysteresis

Integrasi IoT System

Optimal results at a depth of 5 mm pave the way for full integration into the sports IoT ecosystem. The designed integration flow is as follows:

FSR sensors embedded in EVA foam detect changes in resistance due to impact.

a. The microcontroller (e.g. ESP32 or Arduino with Wi-Fi/BLE module) reads analog signals, performs ADC conversion, applies 2.5 ms latency compensation, and calculates peak force estimates.
b. The communication module sends raw data (timestamp, ΔR value, force estimate) to a cloud platform (e.g. Firebase, AWS IoT, or Blynk).
c. The dashboard displays real-time data in the form of graphs, risk indicators, and impact history per training session.

Figure 4. Intelligent Sports Safety System Architecture and Decision Support System (DSS) Integration

An alert can be sent to the coach's smartwatch or athlete's phone if the impact force exceeds a predetermined threshold.

To fill this gap, this study offers in silico computational modeling based on the Element Method until multiphysics is linked. This approach marries the Mooney-Rivlin hyperelastic equation on EVA foam with the piezoresistive formulation of FSR in a single dynamic computing environment. The objectives of the study were: (1) to map the distribution of interface voltage at three sensor depth variations, (2) to assess the electrical response and electromechanical latency to transient impact loads, and (3) to formulate the optimum spatial depth (sweet-spot) for robust and accurate smart shin guard fabrication.

LITERATURE REVIEW

EVA Foam Hyperelastic Dissipation

EVA foam is a thermoplastic cellular elastomer material that is a mainstay in the sports protective equipment industry because it is light in density and its capacity to absorb impact energy in milliseconds (Mills, 2007). Unlike linear elastic materials, EVA foam exhibits a non-linear response to high-strain-rate shock loads that take place in three phases: initial linear cell elasticity, a plateau phase when the polymer cell wall is bent, and a densification phase in which the cell wall collides so that the stiffness increases sharply. This non-linear stress-strain profile is mathematically modeled in continuum mechanics through the hyperelasticity approach (Anderson & Carter, 2024).

To illustrate the almost non-compressive properties of EVA foam, this research uses a two-parameter Mooney-Rivlin strain energy density function, which correlates the deformation energy (W) with the invariant Cauchy-Green tensor:

$$W = C_{10}(\bar{I}_1 - 3) + C_{01}(\bar{I}_2 - 3) + \frac{1}{2}\kappa(J-1)^2$$

dengan $\bar{I}_1$ dan $\bar{I}_2$ adalah invarian regangan isokhorik, C_{10} dan C_{01} konstanta material empiris, κ modulus curah, serta J nisbah volume (Kusuma et al., 2023). Pendekatan ini menjamin perhitungan distribusi disipasi energi yang teliti di seluruh domain pelindung.

FSR Sensor Piezoresistance Principle

FSR sensors are electromechanical transducers that convert mechanical pressure into changes in electrical resistance. Physically, FSR is composed of two layers of rigid polymer film substrate (polyimide or PET) that clamp a layer of conductive polymer ink with the addition of carbon nanoparticles. The mechanism of operation rests on the theory of percolation and the quantum tunneling effect (Hakim, 2023; Garcia et al., 2024). When the impact force presses on the EVA foam and reaches the sensor, the distance between the carbon nanoparticles shrinks, multiplying the percolation path so that the electric current increases and the total resistance decreases (ΔR).

This phenomenon is formalized in electrical continuum mechanics by associating the resistivity tensor ρijρij and the voltage tensor σklσkl through the piezoresistive coefficient matrix ππijkl:

$$\frac{\Delta \rho_{ij}}{\rho_0} = \pi_{ijkl}\sigma_{kl}$$

With the integration of Ohm's Law at the effective volume of VinVin-fed fixed-voltage sensors, the transient resistance of R(t)R(t) can be calculated. This combined formulation allows the characterization of the sensor's dynamic response to mechanical fluctuations during the impact phase (Nugroho & Santoso, 2025).

Incompatibility, Stiffness and Micromechanics of the Interface

The toughest engineering problem in wearable composite systems is bringing two materials together with a very uneven modulus of elasticity. Here, the polyimide sensor substrate has a young modulus of about 2.5 GPa, while the EVA foam matrix has an effective modulus of less than 10 MPa. When these hybrid structures are hit by high-speed Gaussian pulses, the discontinuity of elasticity at the border triggers a shear stress concentration (Lee et al., 2024).

According to cracking mechanics, shear stresses that exceed the fatigue limit or yield limit of polyimide plastics will initiate micro-cracking. In line with the accumulation of training cycles, these cracks propagate and eventually lead to complete delamination of the FSR, thwarting the function of the monitoring device early (Gomez & Silva, 2026; Patel, 2023). Reducing shear stress intensity by determining sensor planting depth is the most basic topology optimization solution.

Hypothesis

Based on the theoretical framework above, the following four hypotheses are proposed:

H1: Increased planting depth (dFSR) significantly lowers the interface shear stress because the thicker the EVA bearing is above the sensor, the more tangential forces are dissipated so that the risk of delamination is reduced.

H2: Greater planting depth negatively correlates with ΔR sensitivity because the strain energy is exponentially muffled by the hyperelastic matrix before it touches the sensor.

H3: The viscoelastic and hyperelastic properties of EVA result in hysteresis that generates a time lag (latency) between the peak of mechanical load and the peak of resistance decline.

H4: There is a single sweet-spot depth point that simultaneously keeps the shear voltage below the plastic yield limit, maintains sufficient signal sensitivity, and minimizes latency for IoT purposes.

METHODOLOGY

Research Design

This study uses a full computational quantitative experiment design with a digital twin model in silico. The simulation was run on COMSOL Multiphysics 6.x using the Finite Element Method (FEM). Transient (Time-Dependent) studies were chosen to be able to solve partial differential equations that govern multiphysical interactions between Solid Mechanics and Electric Currents modules simultaneously in time zones (Alamsyah, 2024; Brown et al., 2025).

Research Variables

The experiment is set to test one independent variable against three bound variables, with the outer variable locked.

a. Independent variable: The depth of planting of the FSR sensor (dFSR) from the outer surface, set at 2 mm, 5 mm, and 8 mm.
b. Bound variables: (1) Maximum interface shear voltage (MPa), (2) Percentage change of transient resistance (ΔR, %), and (3) Electromechanical latency (tlatencytlatency, ms).

Geometry, Materials, and Constitutive Equations

The shin guard system is represented as a 3D domain consisting of a protective foam block and a thin FSR sensor inside. The material properties and constant parameters are compiled in Table 2.

Table 2. Geometry Parameters and Properties of Basic Materials for FEM Simulation

Tabel 1. Parameter Geometri dan Properti Material Dasar untuk Simulasi FEM

Kategori	Parameter	Simbol	Nilai	Satuan
Blok EVA	Panjang × Lebar × Tebal	$p \times l \times t_{EVA}$	100 × 50 × 15	mm
Sensor FSR	Jari-jari area aktif / tebal substrat	r_{FSR}/t_{FSR}	10 / 0,2	mm
Variasi kedalaman		d_{FSR}	2, 5, 8	mm
EVA hiperelastis	Massa jenis / Poisson / C10 / C01	$\rho_{EVA}, \nu, C_{10}, C_{01}$	120 / 0,45 / 0,12 / 0,03	kg/m³, –, MPa, MPa
FSR (polimida)	Modulus Young / massa jenis / R_0 / π	E, ρ_{FSR}, R_0, π	2,5 / 1420 / 100 / $2{,}5\times10^{-9}$	GPa, kg/m³, kΩ, Pa^{-1}

Boundary Conditions and Transient Loads

To mimic physiological conditions, a Fixed Constraint is given to the entire back surface of the EVA block which represents the rigid base of the tibia (Adams, 2024). The electrical terminals are set: 5 V DC at the upper pole of the sensor and 0 V (Ground) at the lower pole. The impact load is applied via the Boundary Load on the protective façade. In order not to create a numerical singularity, the force is not modeled as a step function, but rather as an analytical Gaussian pulse that resembles the actual kick kinematics. The peak force Fpeak=1,500Fpeak=1,500 N with contact duration tp=20tp=20 ms, reaches a maximum at t=10t=10 ms (Evans & Wright, 2025).

Numerical Stability and Solver

The quality of spatial dyskritisation is tested through the Grid Independence Test by monitoring the maximum von Mises voltage (σVM,maxσVM,max) at the material border. The number of elements varies from 50,000 to 300,000. Convergence is considered to be achieved when the deviation is less than 1% (Wang, 2023).

Table 3. FEM Computing and Solution Paramter

Kategori	Parameter	Nilai/Konfigurasi
Waktu	Durasi total / Langkah	50 ms / 0,5 ms
Meshing	Tipe elemen / Ukuran area antarmuka	Free Tetrahedral & Swept Mesh / Extremely Fine
	Jumlah elemen operasional	250.000 (deviasi 0,42%)
Solver	Studi / Algoritma	Time Dependent (MUMPS Direct)
	Toleransi konvergensi relatif	1×10^{-6}

The resolution of 250,000 elements was chosen because it deviates only 0.42% of the 300,000 elements (Chen et al., 2025). The MUMPS solver is used to handle non-linear couplings in small time steps (Nguyen, 2024).

RESEARCH RESULT

Volumetric Damping Testing

The results of mechanical simulations show the superior capacity of EVA foam in reducing trauma. At t=10t=10 ms with a peak load of 1,500 N, the von Mises voltage contour records a maximum concentration of 2.8 MPa in the outer surface area (radius 0–3 mm from the center of impact). This indicates the beginning of compressive buckling on the microcell wall. The shock wave then decays exponentially along the 15 mm thickness of the foam block. On the posterior side in contact with the tibia, the residual stress is reduced to below 0.35 Mpa well below the critical threshold of tibia fracture which is estimated to be around 4,000 N (Adams, 2024). This result confirms the basic protection function of EVA materials.

Electromechanical Parametric Analysis

The core of the study was a parametric sweep to evaluate the effect of planting depth (dFSRdFSR) on structural reliability and signal quality. The summary is presented in Table 3.

Tabel 3. Matriks Kinerja Elektromekanikal pada Variasi Kedalam Sensor (Beban Puncak 1.500 N)

Parameter	2 mm (Dangkal)	5 mm (Sedang)	8 mm (Dalam)
Tegangan geser antarmuka (MPa)	42,5	24,8	12,4
Status risiko kegagalan	Kritis (delaminasi tinggi)	Aman (dalam toleransi)	Sangat aman
Perubahan resistansi ΔR (%)	-85	-62	-25
Latensi elektromekanik (ms)	1,2	2,5	4,8
Kualitas sinyal (SNR)	Tinggi tapi noisy	Sangat baik, linear	Rendah (teredam)

At the 2 mm configuration, the shear stress of 42.5 MPa is already close to the polyimide yield limit (~70 MPa), which is very dangerous for long-term durability (Lee et al., 2024). On the other hand, a depth of 8 mm produces only a ΔR of -25% that is easily submerged in the network noise floor (Rossi & Bianchi, 2025).

The resistance transient response confirms the piezoresistive effect: as the load increases, the distance between the carbon particles narrows so that the ΔR drops sharply. However, the decrease in resistance did not exactly coincide with the peak of mechanical load at t=10t=10 ms. There was a temporal shift: latency of 1.2 ms (2 mm), 2.5 ms (5 mm), to 4.8 ms (8 mm). This latency comes from the viscoelastic relaxation of the EVA polymer chain before the strain reaches the sensor (Hwang & Kim, 2025).

Determination of Sweet-Spot

The simulation results refute the trial-and-error approach. Planting the sensor too shallow does result in maximum sensitivity, but Young's extreme modulus difference triggers a destructive shear voltage spike. Planting too deep is mechanically safe, but it loses its "smart" function because the signal is too weak. Taking into account all aspects, a depth of 5 mm (about 33%–50% of the total thickness of 15 mm) appears as a sweet-spot. In this position, the shear stress is compressed to 24.8 MPa (providing a safety factor >2 to the polyimide yield limit), and the ΔR remains solid at -62% with minimal noise distortion for microcontroller conversion (Suzuki & Tanaka, 2026).

Implications for IoT and Firmware Design

Another important finding from this multiphysics coupling study is the 2.5 ms delay time inherent in the 5 mm sweet-spot configuration. This delay is rarely detected in pure mechanical simulations without an electrical coupling (Hwang & Kim, 2025; Edwards & Smith, 2024). This latency has a direct impact on telemetry software design: the ARM microcontroller firmware algorithm must compensate for EVA hysteresis to avoid peak clipping that can lead to peak force underestimation of up to 15–20% (Thompson, 2023). Without this compensation, the injury early warning system will not function optimally. Thus, the coupled multiphysics approach that produces an optimal depth of 5 mm not only guarantees sensor durability and data quality, but also serves as the foundation for predictive and precise modern sports safety systems.

DSS Advanced Functions

a. **Cumulative impact dose:** The system calculates force integrals over time for a single training session, providing objective metrics regarding shin structural fatigue.
b. **Pattern detection**: With simple machine learning, DSS can identify increased impact frequencies that indicate decreased technique or athlete fatigue.
c. **Digital medical records**: All impact histories are stored and accessible for long-term analysis by the medical team.

Added Value for Users

a. **Coach**: Get an early warning to make substitutions or modifications to the exercise.
b. **Athlete:** Has an objective awareness of the load that his body receives.
c. **Medical team**: Have quantitative data for evidence-based diagnosis and rehabilitation.

Summary of Discussion in the Matrix Table

Table 4. Results of the FSR Sensor Planting Depth Trade-off Parametric Analysis

Sub-bab	Key Parameter	Key Findings	Implications for IoT
Smart Monitoring	FSR, busa EVA	Conversion of impact → electrical signal	The foundation of the active system
Data Processing	ΔR, SNR	Depth 5 mm = best SNR	Accurate data, low false positives
Latency	2.5 ms	Histeresis hiperelastis terukur	Need to compensate for delay in firmware
IoT Integration	M-cloud-dashboard	Arsitektur end-to-end	Ready-to-use for wearable sports tech
DSS	Style threshold	Early detection of injury risk	Added value for athlete safety

CONCLUSIONS AND RECOMMENDATIONS

A multiphysics FEM computational study using COMSOL successfully formulated precision parameters for the smart shin guard. The optimal FSR sensor planting position is at a depth of 5 mm. At these sweet-spot coordinates, the structural integrity of the sensor is maintained (shear voltage is only 24.8 MPa) while the piezoresistive signal remains strong and reliable (ΔR = -62%). These results encourage the development of a physical prototype through 3D printing for in vitro validation with pendulum impact tests. Advanced testing is needed to verify latency deviations and real signal-to-noise limits, while enriching the design literature of modern sports safety instruments..

ADVANCED RESEARCH

Future research could explore the use of alternative damping materials besides EVA foam, such as polyurethane or fluid-viscous dampers, to compare their effectiveness in damping transient loads on shin guards.

ACKNOWLEDGMENT

A big thank you to the leaders, lecturers, and laboratories of the Sports Engineering Study Program of the Sumatra Institute of Technology for their access to computing facilities and constructive discussions.

REFERENCES

Adams, R. (2024). Impact force characteristics in competitive martial arts: a time-frequency analysis. Journal of Sports Sciences, *42*(5), 456–468.

Alamsyah, F. (2024). Pemodelan multifisika elektromekanikal pada material cerdas menggunakan COMSOL Multiphysics. Jurnal Ilmu Komputer dan Informatika, *15*(2), 112–123.

Anderson, L., & Carter, J. (2024). Hyperelastic modeling of Ethylene-Vinyl Acetate foams under high-strain dynamic impacts for sports applications. Materials & Design, *238*, 112685.

Basuki, R., & Wibowo, A. (2023). Pemodelan elemen hingga pada material peredam kejut berbasis polimer untuk aplikasi pelindung olahraga. Jurnal Rekayasa Mesin, *14*(3), 301–312.

Brown, A., Wilson, J., & Taylor, R. (2025). Coupled in silico modeling of piezoresistive sensor networks in protective sports equipment. Computer Methods in Biomechanics and Biomedical Engineering, *28*(2), 145–158.

Chen, H., Liu, Y., & Zhang, W. (2025). Energy dissipation characteristics of cellular polymeric matrices in lower extremity protective gears. Journal of Biomechanics, *160*, 111980.

Davis, M. (2022). Computational evaluation of ground reaction forces and impact attenuation in sports footwear. Sports Engineering, *25*(1), 8.

Edwards, P., & Smith, K. (2024). Transient structural analysis of soccer shin guards: a numerical approach. International Journal of Impact Engineering, *185*, 104825.

Evans, C., & Wright, D. (2025). Establishing quantitative injury thresholds using wearable telemetry during intense athletic training. Sports Medicine, *55*(1), 89–102.

Fernandez, D. (2023). Digital twin frameworks for pre-fabrication analysis of smart wearable devices. IEEE Internet of Things Journal, *10*(12), 10890–10900.

Garcia, M., Lopez, R., & Martinez, C. (2024). Electromechanical characterization and hysteresis compensation of flexible Force Sensitive Resistors. IEEE Sensors Journal, *24*(5), 6120–6130.

Gomez, E., & Silva, R. (2026). Finite element method approaches to mitigate sensor interface delamination under high shear stress. Computational Materials Science, *215*, 111800.

Hakim, L. (2023). Kalibrasi dan pengujian linearitas sensor tekanan film tipis piezoresistif untuk perangkat wearable. Jurnal Nasional Teknik Elektro, *12*(2), 89–98.

Hidayat, T., Wijaya, A., & Saputra, R. (2022). Analisis numerik penempatan optimal sensor tekanan pada struktur hiperelastis terdeformasi besar. Jurnal Rekayasa Sistem, *11*(2), 77–88.

Hwang, J., & Kim, S. (2025). Dynamic response latency of polyamide-based tactile sensors under high-speed compressive loads. Sensors and Actuators A: Physical, *362*, 114876.

Johnson, T. (2022). Design and signal conditioning of low-cost wearable kinetic sensors for athletic monitoring. IEEE Transactions on Instrumentation and Measurement, *71*, 9504010.

Kusuma, D., Pratama, A., & Nugroho, H. (2023). Analisis tegangan-regangan dinamis pada busa polimer menggunakan metode numerik terpadu. Jurnal Teknik Material dan Metalurgi, *8*(1), 34–45.

Lee, C., Kim, J., & Park, S. (2024). Interface stress analysis between rigid printed electronics and hyperelastic polymer substrates. Flexible and Printed Electronics, *9*(1), 015010.

Liu, Y., & Zhao, X. (2026). Optimizing the thickness and density of EVA foams for impact resistance in contact sports. Polymer Testing, *115*, 107750.

Miller, S. (2022). The shift from passive protective gear to active monitoring systems in contact sports. Research in Sports Medicine, *30*(4), 401–415.

Mills, N. J. (2007). Polymer foams handbook: Engineering and biomechanics applications (1st ed.). Butterworth-Heinemann.

Nguyen, V. (2024). Transient multiphysics simulation of impact forces on embedded electronic skins. Applied Mathematical Modelling, *125*, 234–248.

Nugroho, A., & Santoso, B. (2025). Karakterisasi transduser piezoresistif untuk pengukuran beban mekanis dinamis. Jurnal Teknik Fisika dan Instrumentasi, *9*(1), 22–33.

Patel, R. (2023). Evaluating the durability of flexible sensors embedded in shock-absorbing elastomers. Smart Materials and Structures, *32*(4), 045015.

Putra, E., & Wijaya, H. (2026). Rancang bangun purwarupa shin guard terintegrasi IoT untuk deteksi benturan real-time. Jurnal Teknologi Informasi dan Terapan, *14*(1), 45–54.

Roberts, J., Smith, P., & Williams, T. (2024). Kinematic overload and micro-trauma accumulation in elite martial arts athletes: a prospective cohort study. Journal of Sports Sciences, *42*(3), 245–256.

Rossi, L., & Bianchi, G. (2025). Evaluating the spatial depth of integrated tactile sensors in polymer foams to maximize sensitivity. Journal of Applied Physics, *137*(8), 084501.

Suzuki, K., & Tanaka, M. (2026). Signal-to-noise ratio optimization in embedded piezoresistive arrays for sports biomechanics. Measurement Science and Technology, *37*(2), 025101.

Thompson, L. (2023). Translating raw biomechanical impact data into actionable safety protocols for athletic coaches. International Journal of Sports Science & Coaching, *18*(4), 1122–1133.

Wang, Q. (2023). Overcoming trial-and-error in smart material design through advanced computational coupling. Advanced Engineering Informatics, *55*, 101890.